MSc in Photonics PHOTONICS**BCN**

Universitat Politècnica de Catalunya (UPC)
Universitat Autònoma de Barcelona (UAB)
Universitat de Barcelona (UB)
Institut de Ciències Fotòniques (ICFO)

http://www.photonicsbcn.eu

Master in Photonics

MASTER THESIS WORK

Single-pulsed supercontiuum generation in millimeter pieces of a birefringent microstructured silica fiber under femtosecond laser injection.

Josep Pérez Diez

Supervised by Dr. Stefan Haacke, (IPCMS)

Presented on date 8th september 2009

Registered at

Escola Tècnica Superior d'Enginyeria de Telecomunicació de Barcelona

Single-pulsed supercontiuum generation in millimeter pieces of a birefringent microstructured silica fiber under femtosecond laser injection.

Josep Pérez Diez

Institut de physique et chimie des materiaux de Strasbourg, Strasbourg 67034, France.

Abstract. Microstructured optical fibers (MOF) are a new generation of optical fibers that have a huge flexibility on choosing the location of the zero dispersion wavelength, λ_{ZD} which can be chosen to be very close to the visible and even in the visible, allowing soliton propagation in the near infrared. Moreover, the nonlinearity of silica with femtosecond radiation produces a broadening of the spectra, which is called supercontinuum (SC), due to several nonlinear effects, as self phase modulation (SPM), cross phase modulation (XPM), dispersive wave generation and stimulated Raman scattering. I focused my work on the study of visible dispersive waves generated when a special phase matching condition between initial input pulse and some wave in the normal dispersion regime is fulfilled.

1. Introduction

MOF are made up of a hollow structured matrix of a material (or many materials), that leads to an increase of light confinement in the core of the fiber. That provides a larger Kerr nonlinear effect than in conventional fibers. The kind of MOF that concerns us has a solid core which has a higher refractive index than the microstructured cladding, then the light can propagate by internal total reflection. Although the principle of light propagation is the same as in conventional fibers, MOF provide more variability in the dispersion of the fiber and birefringence due to the freedom of choosing the hole size and the distance between them.

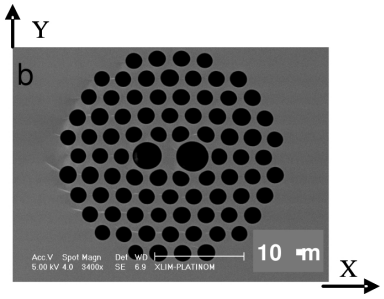

Figure 1. Transversal cut of a birefringent MOF

This experience was performed with a birefringent MOF, whose matrix is made up of fused silica, as the one shown in Figure 1, fabricated in the XLIM laboratory of Limoges, France. It has two bigger holes next to the core, which yield a high birefringence. Such a fiber supports two different propagation modes in the core, which are called LP01 and LP11 that have the anomalous dispersion regime for wavelengths higher than $827nm$ and $757nm$, respectively. In this regime, the dispersion coeficient $D = -\frac{\lambda}{c}\frac{d^2n}{d\lambda^2}$, which is related to the second order coeficient of the Taylor development of the propagation constant‡, is positive, so the chirp induced, $\delta\omega$, will be positive for the leading edge of the pulse and negative for the trailing edge, therefore the higher frequency components will propagate faster than the lower frequencies [1]. On the contrary, as we have a nonlinear medium, the chirp induced due to SPM, will be negative for the leading edge and positive for the trailing edge [1]. So the two effects introduce a change in frequency in two different opposite directions. Therefore it is possible to make a pulse so that the two effects will balance each other. Such pulses are called temporal solitons.

After only $13mm$ of propagation, a phase matching condition takes place between pump beam and some wave of the normal dispersion regime. That yields the formation of a visible dispersive wave close to $600nm$. So we are able, with a $20mm$ fiber piece, to genere a mono-impulsive, ultra-broadband SC with little spectral modulations. Also, with these milimeter pieces of birefringent MOF, the SC achieved and specially the visible dispersive waves are quite different from that of previous related works [5] [7]. The aim of this work is to study the generation of these single-pulsed and ultra-broadband dispersive waves in $20mm$ fiber pieces, in order to use it for implementing a compact transient absorption spectrometer with broadband detection and 150-fs FWHM time resolution, to monitor the ultrafast dynamics of the electronic states of malachite green in ethanol excited to the S2 state [6].

I have made numerical simulations of the nonlinear Schrödinger equation to compare them with the experimental spectra of supercontinuum generated with $50fs$ pulses in a birefringent MOF. The experimental spectra were obtained by the GONLO group of IPCMS for the mode LP01 at different fiber lengths (L) between $0mm$ and $22mm$. I have also obtained the experimental spectra for the mode LP11, and I compared them with the simulations.

2. Theoretichal background

2.1. Generalized nonlinear Schrödinger equation (GNLSE) and soliton propagation

The propagation of optical fields in fibers is governed by Maxwell's equations which are used to obtain the wave equation

$$\nabla \times \nabla \times \mathbf{E} = -\frac{1}{c^2}\frac{\partial^2 \mathbf{E}}{\partial t^2} - \mu_0 \frac{\partial^2 \mathbf{P}}{\partial t^2} \tag{1}$$

‡ The propagation constant is defined as follows: $\beta(\omega) = n(\omega)\frac{\omega}{c}$, where n is the refractive index and c is the speed of light

To complete the description, a relation between the induced polarization $\mathbf{P}$ and the electric field $\mathbf{E}$ is needed. Although the quantum mechanical approach for evaluating of $\mathbf{P}$ is often necessary when the optical frequency is near a medium resonance, a phenomenological relation of the form

$$\mathbf{P} = \varepsilon_0 \left(\chi^{(1)} \cdot \mathbf{E} + \chi^{(2)} : \mathbf{EE} + \chi^{(3)} \vdots \mathbf{EEE} + \cdots \right) = \mathbf{P}_L + \mathbf{P}_{NL} \tag{2}$$

can be used to relate $\mathbf{P}$ and $\mathbf{E}$ for optical fibers in the wavelength range $0.5 - 2\mu m$, far from medium resonances, for the study of nonlinear effects. Where $\mathbf{P}_L$ is the linear term of the expression and $\mathbf{P}_{NL}$ includes the remaining nonlinear terms.

For ultrashort pulses, bellow 100fs, and taking into account just the third order nonlinear term of the eq. 2 one can obtain, by developing the eq. 1 for z axis propagation, the envelope nonlinear equation or generalized nonlinear Schrödinger equation [1]

$$\left[\frac{\partial}{\partial z} - \hat{D} + \frac{\alpha}{2} \right] A(z,T) = i\gamma(\omega_0) \left(1 + i\tau_{shock} \frac{\partial}{\partial T} \right) \times$$
$$A(z,T) \int_{-\infty}^{\infty} R(\tau_1) |A(z, T-\tau_1)|^2 d\tau_1 \tag{3}$$

where $A(z,T)$ is the envelope complex amplitude of the propagating field, in a frame of reference traveling at group velocity of the input pulse§. The latter is defined as

$$\tilde{E}(\mathbf{r}, \omega - \omega_0) = F(x,y) \tilde{A}(z, \omega - \omega_0) exp(i\beta_0 z) \tag{4}$$

where $F(x,y)$ is the transverse modal distribution and $\tilde{E}$ is the Fourier transform of E defined as

$$\tilde{E}(\mathbf{r}, \omega) = \int_{-\infty}^{+\infty} E(\mathbf{r}, t) exp(i\omega t) dt \tag{5}$$

The remaining terms in eq. 3 are the following:

- $\hat{D} = \sum_{m \geq 2} \frac{i^{m+1}}{m!} \left(\frac{\partial^m \beta}{\partial \omega^m} \right)_{\omega=\omega_0} \frac{\partial^m}{\partial T^m}$ is an operator that accounts for dispersion
- α is the loss coeficient. $[\alpha] = m^{-1}$
- $\gamma(\omega_o) = \frac{n_2(\omega_0)\omega_0}{c A_{eff}(\omega_0)}$ is the nonlinear parameter [1]. $[\gamma] = m^{-1}W^{-1}$.
- $\tau_{shock} = \tau_0 - \frac{\partial}{\partial \omega} [ln A_{eff}(\omega)]_{\omega=\omega_0}$ describes the frequency dependence of the guided mode on the effective area. The temporal derivative represents the self-steepening effect [2]
- The convolution integral describes the Raman response of the fiber. The function $R(\tau_1)$ describes both the instantaneous and delayed material response:

$$R(\tau_1) = (1 - f_r)\delta(\tau_1) + f_r h_r(\tau_1), \tag{6}$$

§ $T = t - \frac{z}{v_g}$, where v_g is the group velocity

where $\delta(\tau_1)$ and h_r are the instantaneous and delayed Raman responses, respectively, and they can be expressed with good accuracy by an analytical function reported in Ref. [3]. $f_r = 0.18$ represents the contribution factor.

Eq. 3 is a nonlinear partial differential equation. One of the most used methods to solve it is the well known split-step Fourier method. This allows to write equation 3 as

$$\frac{\partial A}{\partial z} = (\hat{D} + \hat{N})A \tag{7}$$

where $\hat{D}$ and $\hat{N}$ are the dispersion and nonlinear differential operators, respectively. Such a numerical method assumes that in propagating the optical field over a small distance h, the dispersive and nonlinear effects can be pretended to act independently. More specifically, propagation from z to $z + h$ is carried out in two steps. In the first step, the nonlinearity acts alone, and $\hat{D} = 0$ and in the second step, dispersion acts alone, and $\hat{N} = 0$ [1]. Although the method is relatively straightforward to implement, it requires that step sizes in z and T are small enough to maintain the required accuracy.

Also eq. 3 can be analytically solved when all parameters are set to zero except β_2 and γ. In this case, the exact solution is a soliton, which is a special solution of eq. 3 when only 2nd order of dispersion and nonlinear terms are accounted for. In this experience we are focused only in fundamental solitons ($N = \frac{\gamma P_0 {T_0}^2}{|\beta_2|} = 1$) [1].

2.2. Nonlinear effects

For an intense light-matter interaction with some dielectric materials, as silica, the $\chi^{(3)}$ term of eq. 2 is responsible for different processes such as stimulated Raman scattering, four wave mixing and optical Kerr effect. The first one is responsible for RSFS. For four wave mixing to be observed it is necessary to satisfy a phase-matching condition inside the fiber, which is not automatically fulfilled. Optical Kerr effect arrises from the intensity dependence of refractive index and it is responsible for SPM and XPM.

The basic idea of SPM is that refractive index intensity dependence in nonlinear materials produces a phase variation in the pulse that propagates through the latter, which leads to spectral broadening since the different frequencies of the pulse will propagate at different velocities, as happened with dispersion.

XPM is always accompanied by SPM but the former occurs when more than one waves copropagate inside the fiber, so refractive index of a wave depends not only on the intensity of that wave but also on the intensity of the other copropagating waves, acquiring an intensity dependent nonlinear phase given by [1]

$$\phi_j^{NL} = \frac{\omega_j z}{c}\Delta n_j = \frac{\omega_j z n_2}{c}\left[|E_j|^2 + 2|E_{3-j}|^2\right] \tag{8}$$

where $j = 1$ or 2. The first term is responsible for SPM and the second term results from phase modulation of one wave by the copropagating wave and is responsible for XPM. The factor of 2 in the second term of the right-hand side of equation 8 shows that XPM is twice as effective as SPM for the same intensity.

RSFS consists of an energy transfer from higher frequency components of the pulse to the lower ones, this is because in fused silica the Stokes processes dominate contrary to anti-Stokes processes [8].

Stimulated Raman scattering and optical Kerr effect are the dominant effects in SC generation.

2.3. Dispersive wave generation

Inside the fiber, the input pulse is first temporally compressed, so spectrally broadened. Therefore at some distance latter in the fiber, the spectral overlap between initial pump pulse and some dispersive wave (DW) with the same wavevector as initial pulse can generate a visible DW peak. The location of the latter in the spectrum can be found from the specital phase matching condition [5]

$$\Delta\beta = (1 - f_R)\gamma(\omega_p)P_p - \sum_{n\geq 2} \frac{(\omega_{DW} - \omega_P)^n}{n!}\beta_n(\omega_p) = 0 \tag{9}$$

where P_p is the peak power of compressed pulse (and not to that of the initial input power), which is roughly doubled after compression [1].

3. Experimental setup

For the spectra measurements I used the setup represented in figure 2. There is a femtosecond laser that gives $\tau_{pulse} = 50fs$ pulses with a frequency of $\nu_{laser} = 27MHz$ at $840nm$, horizontally polarized with regard to the optical table. Then there is a half waveplate and a beam splitter whose reflectivity depends on the polarization axis of incident light, so by turning the half waveplate we can change the power of the beam. The beam splitter was also used to send part of the beam to another experiment. Afterwards, a mirror send the beam to another half waveplate that is used for changing the polarization axis orientation of the beam. The beam splitter just before the microscope objective was used to send the reflected beam, comming from the fiber, towards a camera, in order to see where the beam is hitting the fiber and also to see a transversal section of the fiber when the latter is illuminated. The fiber spectrometer was used to measure the spectra.

I measured the average power at the input of the fiber and I obtained $P_M = 27mW$, so the average energy for one pulse is $E_M = \frac{P_M}{\nu_{laser}} \simeq 9.6 \cdot 10^{-10}J$, and the peak power is $P_p = \frac{E_M}{\tau_{pulse}} = 20KW$.

The fiber is placed onto a translation stage which can be displaced in x, y and z directions by three micrometer screws. In this way you can select where the laser beam is launched into the fiber.

The fiber spectrometer covers a wavelength range from $300nm$ to $850nm$, which is the interest interval of our study of visible dispersive waves. However I've only used it for measuring the experimental SC spectra for the mode $LP11$, the other spectra,

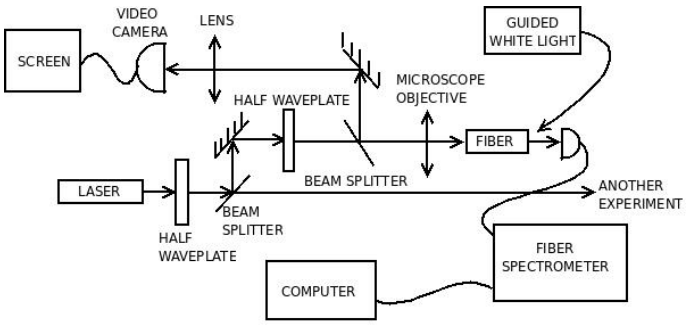

Figure 2. Experimental setup

regarding the mode LP01, were obtained by N. Lecong, a PhD student, using a CCD camera in the wavelength range from $500nm$ to $1100nm$.

4. Results and discussion

Figure 3 shows the two different modes supported in the core of the fiber, LP01 and LP11, which are the fundamental and first excited linearly polarized electromagnetic modes. The photos were taken at the output of the fiber on a screen placed $5cm$ behind the fiber.

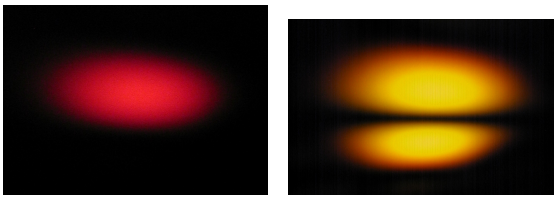

(a) Mode $LP01_x$ (b) Mode $LP11_x$

Figure 3. Supported modes in the core of the fiber.

In fact, since the fiber is highly birefringent, 4 distinct core modes can be guided, $LP01_x$, $LP01_y$, $LP11_x$ and $LP11_y$. Figure 4 shows the dispersion curves for each one of them [4].

With the 2nd half waveplate of Figure 2, I chose to excite only $LP01_x$ and $LP11_x$ modes, which has the zero dispersion wavelength (the wavelength at which dispersion vanishes, λ_{ZD}) at $827nm$ and $757nm$, respectively.

In order to give a physical explanation of the phenomena that yield the observed spectral broadening at the output of the fiber, it's worth looking at the calculated time-resolved spectra diagram. I used a program made by A. Tonello, from XLIM, for solving the GNLSE and made simulations of the spectra at the ouput of the fiber for different lengths, using the same conditions as the experimental spectra. Figure 5 shows these time-resolved spectra at different lengths of the fiber, for $LP01_x$ mode. In this figure we observe that the input pump beam spectrally broaden and splits into two waves, one in the nomal dispersion regime and the other in the anomalous one. The former

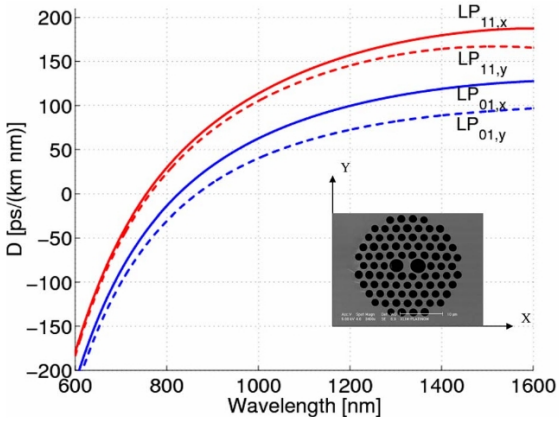

Figure 4. Numerically calculated dispersion coefficient for the first two spatial modes of the MOF.

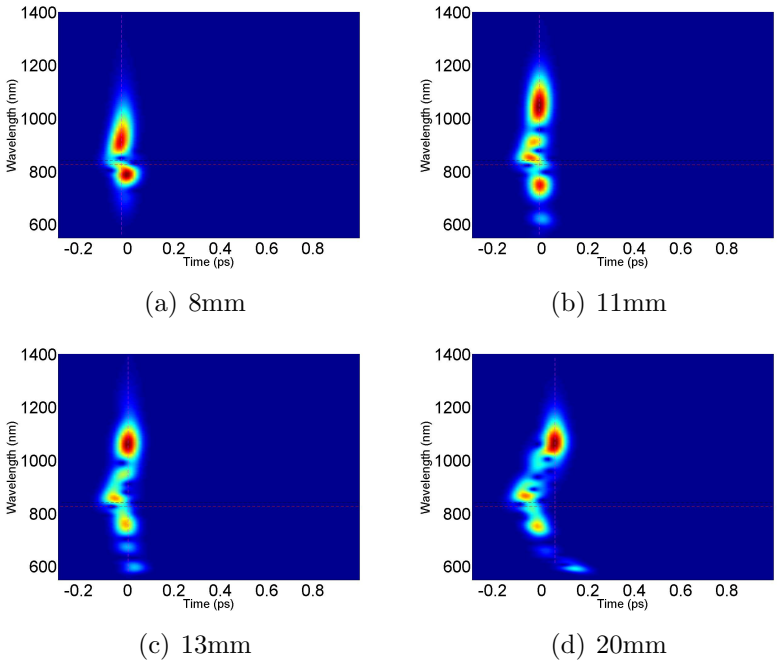

(a) 8mm (b) 11mm

(c) 13mm (d) 20mm

Figure 5. Time-resolved spectra at different fiber lengths for $LP01_x$ mode. Black dashed line shows the pump wavelength, red dashed line represent the λ_{ZD} wavelength and magenta dashed line (vertical) is just to show which is the visible part of the spectra that copropagates with the soliton.

propagates slower than the latter because of the change of dispersion regime. As the length of the fiber increases these waves shift both spectrally and temporally. At $11mm$ is generated a new wave in the visible part of the spectra which propagates slower than the rest of the spectral components.

As we can see in figure 5(a) the input pulse initially centered at $840nm$ is spectrally broadened due to SPM and stimulated Raman scattering. Part of this now broadened input pulse propagates with the normal dispersion, and will be potentially delayed.

Afterwards, in figures 5(b) one can observe this new visible wave generated close to $600nm$ due to the fulfilled phase matching condition, which says that some wavelengths in the normal dispersion regime can propagate with the same β as the pump beam. This defines the DW, a narrow peak in the visible. After spectral broadening, part of the blue wing of the input pulse falls into this wavelength window and co-propagates now, as normal dispersive, with the same beta as the original pulse at 840 nm. One observes an intensity enhancement for these wavelengths close to $600nm$ [5].

At the same time, the input pulse converts into a soliton which progressively red-shifts due to stimulated Raman scattering. One can clearly see that most of the initial input pulse energy is now concentrated around $1000nm$. This soliton interacts with the rest of SC by XPM while copropagation exists, as one can observe in figures 5(c) and 5(d).

To prove the dispersive wave physical origin of this peak generated in the visible, phase matching condition of eq. 9 has been solved to find which are the wavelengths that fulfill it. I have obtained $\lambda_{DW} = 607nm$, which is really close to the observed dispersive wave in figure 5.

Similar evolution occurs for $LP11_x$ mode. Figure 6 shows the time-resolved spectra.

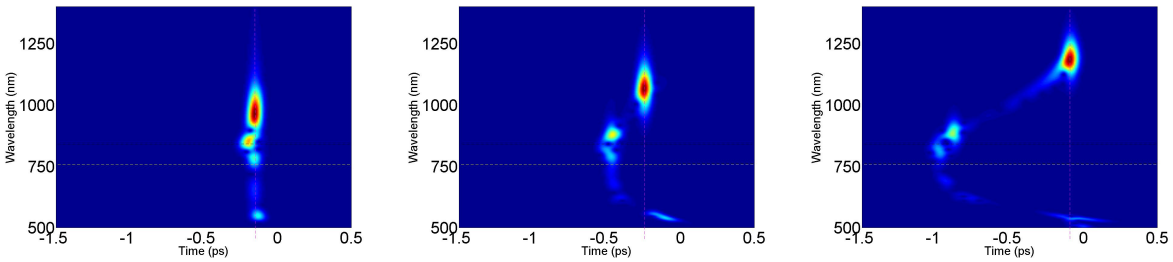

(a) 8mm (b) 20mm (c) 40mm

Figure 6. Time-resolved spectra at different fiber lengths for $LP11_x$ mode. Black dashed line shows the pump wavelength, red dashed line represent the λ_{ZD} wavelength and magenta dashed line (vertical) is just to show which is the visible part of the spectra that copropagates with the soliton.

As in the $LP01_x$ mode, in figure 6(a) we see that the initial pulse has split into two separated peaks due to SPM. However for $LP11_x$ these two separated peaks travels in the anomalous dispersion regime, since now λ_{ZD} is located at $757nm$. Also, there is soliton propagation and the dispersive wave generated in the visible, now close to $550nm$. As the soliton shifts to the red, since it is in the anomalous dispersion regime, its group velocity decreases, therefore the red-shifted spectral components of dispersive wave catch up with the soliton. As a result, the latter interacts with dispersive wave by XPM, generating a new peak with higher frequency, which can be seen in figure 6(c). The XPM induced by dispersive wave in soliton is negligible, as it is seen in the spectra.

Figure 7 shows a comparison between experimental and simulated spectra for $LP01_x$ and $LP11_x$ modes, respectively.

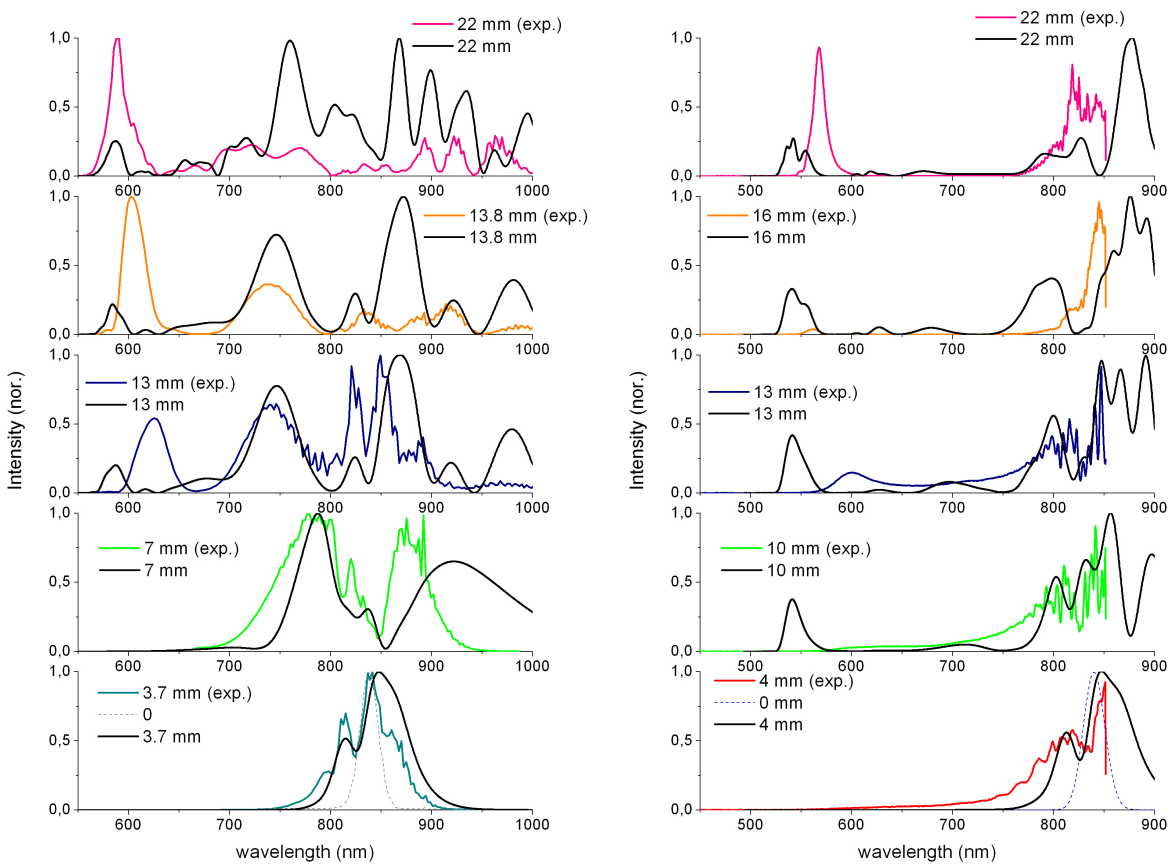

(a) Comparison between experimental and simulated spectra at the ouput of the fiber for different fiber lengths, for the $LP01_x$ mode.

(b) Comparison between experimental and simulated spectra at the ouput of the fiber for different fiber lengths, for the $LP11_x$ mode.

Figure 7. Experimental and simulated spectra for $LP01_x$ and $LP11_x$ modes

We can observe for $LP01_x$, although the intensities are not in a good agreement, that there is a good agreement between experiments and simulations. Discrepancies in the peak intensities can be partly reduced if the detectors response function is accounted for.

The purpose of the comparison with experiment is to validate the simulations. The latter then allow explaining why we were unable to get more blue SC under the present conditions, and they allow to predict what will happen if we change parameters such as pump power, polarisation and wavelength.

Such a result helps us understanding the formation of the SC, and may allow us predicting the ideal fiber parameters for the generation of broadband, single pulsed SC to be used for spectroscopy.

5. Conclusion

The SC genareation in *mm* MOF pieces under sub-50 fs pulse excitation has been simulated, and a simplified explanation of the non-linear processes involved has been given. Most of these important spectral and temporal features predicted for the LP01x mode were observed experimentally. The simulations give now a rationale for the observations, and allow to predict the blue-most extension of the SC as a function of parameters such as pump wavelength, pump power and the selected transverse mode.

6. Acknowledgments

I want to acknowledge my tutor Stefan Haacke and Nhan Lecong, for helping me to understand several concepts regarding fiber optics and for beeing with me in the laboratory when I needed. Also I acknowledge Alexis Labruyere, from the XLIM institut (Limoges, France), for all his help with the explanation of nonlinear effects and for his help with the simulation matlab program, and Philippe Leproux, from XLIM, for their support and for encouraging me when it seems that the results were not quite good. I also want to acknowledge Alessandro Tonello who made the matlab code.

References

[1] Govind P. Agrawal: *Nonlinear fiber optics*, Academic press (1995).

[2] F. DeMartini, C. H. Townes, T. K. Gustafson, and P. L. Kelley. *Self-Steepening of light pulses.* Phys. Rev. **164**, 312-323 (1967)

[3] K. Blow, D. Wood, *Theoretical description of transient stimulated Raman scattering in fibers*, IEEE J. of Quantum Electronics **25**, 2665-2673 (1989).

[4] C. Lesvigne *et. al.*, *Visible supercontinuum generation controlled by intermodal four-wave mixing in microstructured fiber*, Optics letters textbf32, 2173-2175 (2007).

[5] G. Genty, M. Lehtonen, and H. Ludvigsen *Effect of cross-phase modulation on supercontinuum generated in microstructured fibers with sub-30 fs pulses*, Optics express **12** 4614 (2004)

[6] Jérémie Léonard *et. al. Broadband ultrafast spectroscopy using a photonic crystal fiber: application to the photophysics of malachite green*, Optics express **15** 16124 (2007)

[7] John M. Dudley *et. al. Supercontinuum generation in photonic crystal fiber*, Reviews of modern physics, **78** (2006)

[8] F. M. Mitschke and L. F. Mollenauer *Discovery of the soliton self-frequency shift*, Optics letters, **11** 669 (1986)